

Effect of the mediator in feedback mode-based SECM interrogation of indium tin-oxide and boron-doped diamond electrodes

A. K. Neufeld · A. P. O'Mullane

Received: 26 April 2006 / Revised: 26 April 2006 / Accepted: 23 May 2006 / Published online: 20 July 2006
© Springer-Verlag 2006

Abstract Indium tin-oxide (ITO) and polycrystalline boron-doped diamond (BDD) have been examined in detail using the scanning electrochemical microscopy technique in feedback mode. For the interrogation of electrodes made from these materials, the choice of mediator has been varied. Using $\text{Ru}(\text{CN})_{6(aq)}^{4-}$, ferrocene methanol (FcMeOH), $\text{Fe}(\text{CN})_{6(aq)}^{3-}$ and $\text{Ru}(\text{NH}_3)_{6(aq)}^{3+}$, approach curve experiments have been performed, and for purposes of comparison, calculations of the apparent heterogeneous electron transfer rates (k_{app}) have been made using these data. In general, it would appear that values of k_{app} are affected mainly by the position of the mediator reversible potential relative to the relevant semiconductor band edge (associated with majority carriers). For both the ITO (n type) and BDD (p type) electrodes, charge transfer is impeded and values are very low when using FcMeOH and $\text{Fe}(\text{CN})_{6(aq)}^{3-}$ as mediators, and the use of $\text{Ru}(\text{NH}_3)_{6(aq)}^{3+}$ results in the largest value of k_{app} . With ITO, the surface is chemically homogeneous and no variation is observed for any given mediator. Data is also presented where the potential of the ITO electrode is fixed using a ratio of the mediators $\text{Fe}(\text{CN})_{6(aq)}^{3-}$ and $\text{Fe}(\text{CN})_{6(aq)}^{4-}$. In stark contrast, the BDD electrode is quite the opposite and a range of k_{app} values are observed for all mediators depending on the position on the surface. Both electrode surfaces are very flat and very

smooth, and hence, for BDD, variations in feedback current imply a variation in the electrochemical activity. A comparison of the feedback current where the substrate is biased and unbiased shows a surprising degree of proportionality.

Keywords Scanning electrochemical microscope · Indium tin-oxide · Boron-doped diamond · Mediator · Feedback mode

Introduction

Use of the scanning electrochemical microscope (SECM) is becoming more commonplace in the disciplines of biology, chemistry and materials [1–18]. Both feedback mode and substrate generation–tip collection mode and theory are well developed for many electroanalytical applications [19–24]. Central to all SECM experiments is the appropriate choice of a suitable mediator. In many instances it is desirable that the mediator remains innocent; however, in some cases a highly localised and controlled modification of a material's surface is possible [18, 25–28].

New electrode materials like boron-doped diamond (BDD) [26, 29–36] and indium tin-oxide (ITO) [37–39] are of considerable interest in the fields of electroanalytical chemistry, electrochemical technology and solid state electronics. Perhaps one of the most important uses of ITO is in the construction of flexible organic light emitting diodes [39, 40]. BDD on the other hand has received much attention because of its wide operating potential, stability in a wide range of solvent and electrolyte conditions and overall robustness [32]. Details not observed by conventional voltammetry have been uncovered by the specific chemical treatment of ITO and BDD surfaces [31]. Specifically for BDD, it has been shown

Dedicated to Alan, a good friend and colleague on his 60th birthday.

A. K. Neufeld (✉)
BlueScope Steel Research,
P.O. Box 202, Old Port Rd, Port Kembla 2505,
New South Wales, Australia
e-mail: Aaron.Neufeld@bluescopesteel.com

A. P. O'Mullane
School of Chemistry, Monash University,
Clayton, Victoria 3800, Australia

that chemical treatments affect the voltammetry response of certain analytes and surface-adsorbed species [26, 41]. H-terminated surfaces show much higher values of the heterogeneous electron transfer rate constant for ferri/ferrocyanide in comparison to O-terminated surfaces [42]. Characterisation of ITO and BDD electrodes has been performed with conventional cyclic voltammetry (CV) by many groups; however, uncompensated resistance makes the interpretation of data for a heterogeneous rate transfer constant difficult. In addition, the CV technique poorly resolves the effects that heterogeneity may play in the voltammetric response. For both electrode materials, the electronic and physical structure and the chemistry of the semiconductor's surface have an important influence on electron transfer kinetics [37, 38, 43–45]. Hence, the opportunity exists to understand these materials by the use of the SECM method, which is ideally suited to probe the localised surface electrochemical activity of these materials.

In this paper, special attention is given to exploring the effect of different mediators in the feedback mode of SECM-based interrogation of ITO and BDD electrodes. To be specific, we have almost exclusively used feedback mode under the conditions where no potential control of the substrate is implemented to enhance the subtleties of surface-controlled charge transfer kinetics. In feedback mode SECM, a mediator species O that normally undergoes a highly reversible electrochemical reaction is reduced at the ultra-microelectrode (UME) at a diffusion-controlled rate according to the following equation:



The rate of regeneration of the mediator O at the substrate via the reverse reaction of Eq. 1 governs the extent of the positive or negative feedback and provides information on the electron transfer kinetics at the substrate. This rate can be controlled by the potential of the substrate, which can be done either by connection to a potentiostat or by controlling the concentration ratio of redox species (O and R) in solution. Feedback mode may also be conducted where the oxidised form of the mediator is generated at the UME, and the same type of response is observed. An illustration in Fig. 1 shows how the feedback effect is achieved for both an oxidation and reduction process at the substrate. We have used the mediators $\text{Ru}(\text{CN})_{6(aq)}^{4-}$, FcMeOH , $\text{Fe}(\text{CN})_{6(aq)}^{3-}$ and $\text{Ru}(\text{NH}_3)_{6(aq)}^{3+}$ in aqueous electrolyte in an attempt to probe the influence of the semiconductor electronic structure on charge transfer behaviour between the electrode's surface and the mediator. Unless explicitly stated, the ITO and BDD electrodes are interrogated at their open circuit potential (OCP). At OCP, it is anticipated that the broad range of mediator reversible potential (see Table 1) will have an effect on the regeneration of the mediator because of effects on the space

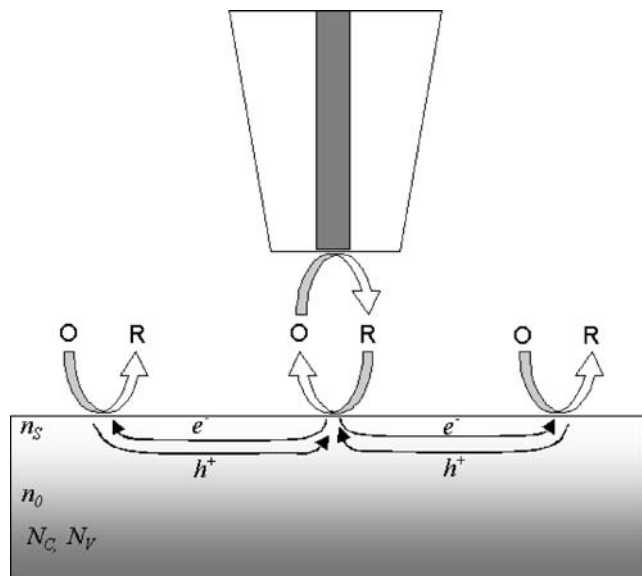


Fig. 1 Diagram depicting the interaction of a mediator (O/R) with a semiconductor surface in feedback mode SECM. Within the semiconductor surface, the *lightly shaded region* represents the space charge layer. For the n (p) type semiconductor, electrons (e^-) [holes (h^+)] will be the majority charge carrier and migrate as shown to maintain charge neutrality. n_S represents the concentration of charge carriers at the surface and n_0 represents those in the bulk of the semiconductor material. N_C (N_V) is the density of states in the conduction (valence) band

charge layer. To more subtly vary the potential at the ITO–electrolyte interface, mixtures of $\text{Fe}(\text{CN})_{6(aq)}^{3-}$ and $\text{Fe}(\text{CN})_{6(aq)}^{4-}$ have been systematically varied. Specific attention has also been given to data relating to the chemical heterogeneity of the BDD electrode and exploring the relationship between data collected at open circuit and biased conditions.

Experimental

Materials and chemicals

Analytical-grade potassium ferricyanide $\text{K}_3\text{Fe}(\text{CN})_6$, hexaammineruthenium (III) chloride $\text{Ru}(\text{NH}_3)_6\text{Cl}_3$, potassium hexacyanoruthenate (II) hydrate $\text{K}_4\text{Ru}(\text{CN})_6 \cdot \text{H}_2\text{O}$, KNO_3 , ferro-

Table 1 Reactions describing the interaction of electrogenerated species with the ITO and BDD electrode surface and their standard reversible potential [35, 48]

Reaction	Standard potential [V vs NHE]
$\text{Ru}(\text{CN})_{6(aq)}^{3-} + e^- \rightleftharpoons \text{Ru}(\text{CN})_{6(aq)}^{4-}$	0.860
$\text{FcMeOH}_{(aq)}^+ + e^- \rightleftharpoons \text{FcMeOH}_{(aq)}$	0.400
$\text{Fe}(\text{CN})_6^{4-} \rightleftharpoons \text{Fe}(\text{CN})_{6(aq)}^{3-} + e^-$	0.358
$\text{Ru}(\text{NH}_3)_{6(aq)}^{2+} \rightleftharpoons \text{Ru}(\text{NH})_{6(aq)}^{3+} + e^-$	0.045

cenemethanol (FcMeOH), acetone, propan-2-ol and acetonitrile were used as received from Aldrich. All aqueous solutions were prepared from water (resistivity 18.2 MΩ cm) purified by a Milli-Q reagent deioniser (Millipore). Degassing of solutions was performed using Argon. BDD electrodes where obtained from Windsor Scientific and ITO-coated glass ($10 \Omega \text{ sq}^{-1}$) from Precision Glass and Optik. Prior to SECM inspection, the electrodes were rinsed in deionised (DI) water, isopropanol, DI water again and then dried under a stream of nitrogen. For experiments on ITO, new electrodes were used for each of the different mediators. When performing feedback approach curve experiments under potential control, the electrodes were mounted in a home constructed cell. Electrical connection was made with the aid of silver-loaded epoxy (ITO) or indium gallium eutectic (BDD).

Procedures and instrumentation

SECM measurements were carried out with a CH Instruments model CHI 900 electrochemical analyser. The two-electrode configuration consisted of a 2-, 10- or 25-μm-diameter Pt UME and a silver wire quasi-reference electrode (AgQRE). However, for OCP and potential control experiments, a three-electrode configuration was employed, which consisted of a Pt UME working electrode, a Pt wire auxiliary electrode and an Ag|AgCl (3 M KCl) reference electrode. The mediators selected for this study were ferrocenemethanol (FcMeOH), Ru(NH₃)₆Cl₃, K₄Ru(CN)₆ and K₃Ru(CN)₆, all in aqueous 0.1 M KNO₃ supporting electrolyte. All approach curve experiments were carried out at an approach rate of 1 μm s⁻¹. Feedback mode imaging was performed by rastering the UME at a constant height above the substrate. Electron microscopy images were obtained with a Philips XL30 field emission gun scanning electron microscope, while energy-dispersive X-ray spectra were collected using an Oxford Link energy dispersive spectroscopy system. Surfaces were imaged using accelerating voltages between 2 and 12 keV, using both backscatter and secondary electron detectors. In most instances, images were obtained on uncoated specimens using a 3-keV accelerating voltage and the smallest spot size available on this model of instrument. Atomic force microscopy (AFM) was performed in tapping mode using a Digital Instruments Multimode AFM with Extender electronics and a Nanoscope IIIa controller.

Approximation of k_{app} by analysis of approach curve data

It is intended in this paper to compare approach curve data obtained from each mediator. For each of the mediators in this study, the apparent heterogeneous electron transfer rate constant (k_{app}) may be calculated by fitting the experimental SECM approach curves to the theory developed by Bard

[22, 35, 46–48]. Even though this analysis is not intended for electrodes of the type used in this study, it seems reasonable in the present study to use this analysis to semi-quantitatively compare the results.

In Bard's theory [46], approach curves are described by the finite current I_T^K , which is derived via the expression in Eq. 2:

$$I_T^K(L) = I_S \left(1 - I_T^{INS} / I_T^C \right) + I_T^{INS} \quad (2)$$

where I_S is the substrate current, and I_T^C and I_T^{INS} represent terms associated with the tip current for diffusion controlled regeneration of the mediator and insulating behaviour, respectively. These terms can be described by the following analytical expressions

$$\begin{aligned} I_S &= 0.78377 / L(1 + 1/\Lambda) \\ &+ [0.68 + 0.3315 \exp(-1.0672/L)] / [1 + F(L, \Lambda)] \end{aligned} \quad (3)$$

$$I_T^C = 0.68 + 0.78377 / L + 0.3315 \exp(-1.0672/L) \quad (4)$$

$$I_T^{INS} = 1 / [0.292 + 1.5151 / L + 0.6553 \exp(-2.4035 / L)] \quad (5)$$

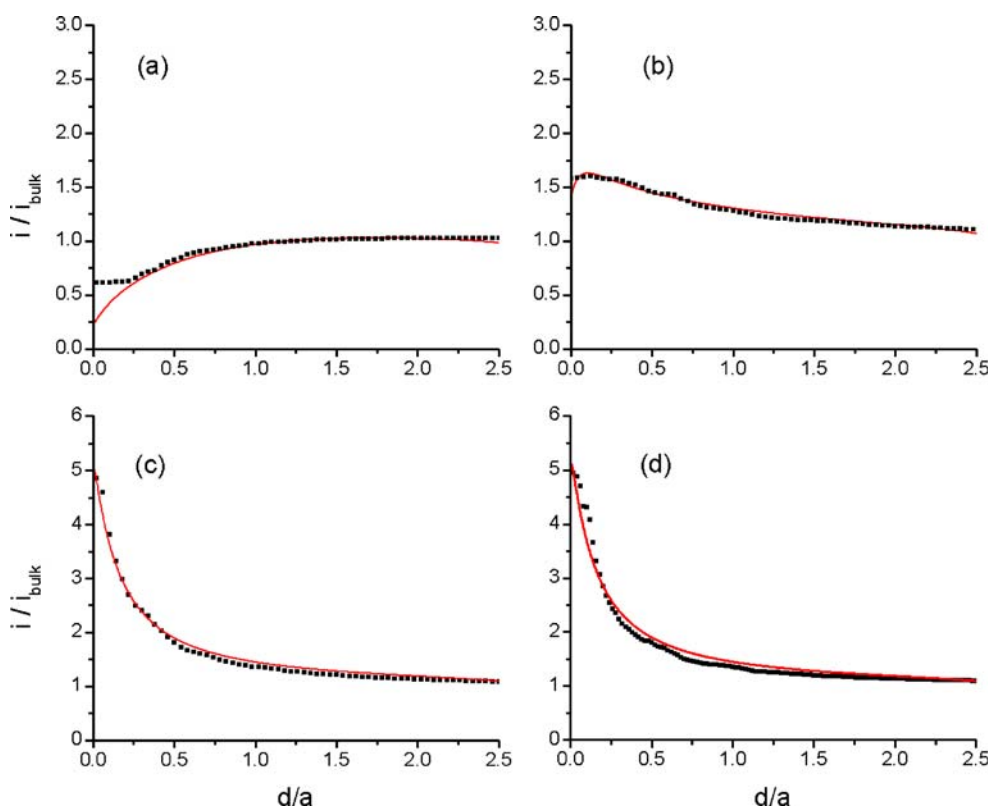
where $L=d/a$ (d is the UME–substrate separation, a is the UME radius), $F(L, \Lambda) = (11/\Lambda + 7.3) / (110 - 40L)$ and $\Lambda = k_{\text{app}} a L / D$, and D is the diffusion coefficient of the mediator. In this study, values of D for each mediator have been determined experimentally using the steady state current at the UME. The values obtained are as follows: FcMeOH $7.0 \times 10^{-6} \text{ cm}^2 \text{ s}^{-1}$, Ru(NH₃)₆³⁺, $9.6 \times 10^{-6} \text{ cm}^2 \text{ s}^{-1}$, Fe(CN)₆⁴⁻_(aq) $6.0 \times 10^{-6} \text{ cm}^2 \text{ s}^{-1}$ and Ru(CN)₆⁴⁻ $5.7 \times 10^{-6} \text{ cm}^2 \text{ s}^{-1}$.

Results and discussion

Variation of the mediator on ITO

If the substrate is at a potential moderately more positive than the mediator standard potential (E°), the generation of the original form of the mediator O should be diffusion controlled and give rise to a pure positive feedback current at the tip described by Eq. 4. It is immediately apparent that at OCP conditions a feedback effect like that for a conductor was not achieved. Data from approach curve experiments performed on ITO and BDD (at OCP) using different mediators are shown by Figs. 2 and 3, respectively, and Table 2 summarises the values of k_{app} obtained from fitting the curves to Eq. 2 (modelled approach curves are also shown in each figure). Figure 2 shows approach curves to ITO for each of the mediators. Very little variation in the

Fig. 2 Approach curve data on ITO using the mediators FeMeOH (**a**), $\text{Fe}(\text{CN})_{6(aq)}^{3-}$ (**b**), $\text{Ru}(\text{CN})_6^{4-}$ (**c**) and $\text{Ru}(\text{NH}_3)_6^{3+}$ (**d**) at a concentration of 1 mM. Obtained using a 10- μm Pt UME at an approach rate of 1 $\mu\text{m s}^{-1}$ in 0.1 M KNO_3 . Modelled approach curves are shown in solid line



approach curve data was observed for repeated approaches to different locations, and values of k_{app} typically varied

less than 10%. The values of k_{app} obtained were 0.073, 0.004, 0.021 and 0.125 cm s^{-1} for the mediators, in the

Fig. 3 Approach curve data on BBD using the mediators FeMeOH (**a**), $\text{Fe}(\text{CN})_{6(aq)}^{3-}$ (**b**), $\text{Ru}(\text{CN})_6^{4-}$ (**c**) and $\text{Ru}(\text{NH}_3)_6^{3+}$ (**d**) at a concentration of 1 mM. Obtained using a 10- μm Pt UME at an approach rate of 1 $\mu\text{m s}^{-1}$ in 0.1 M KNO_3 . Modelled approach curves are shown in solid line

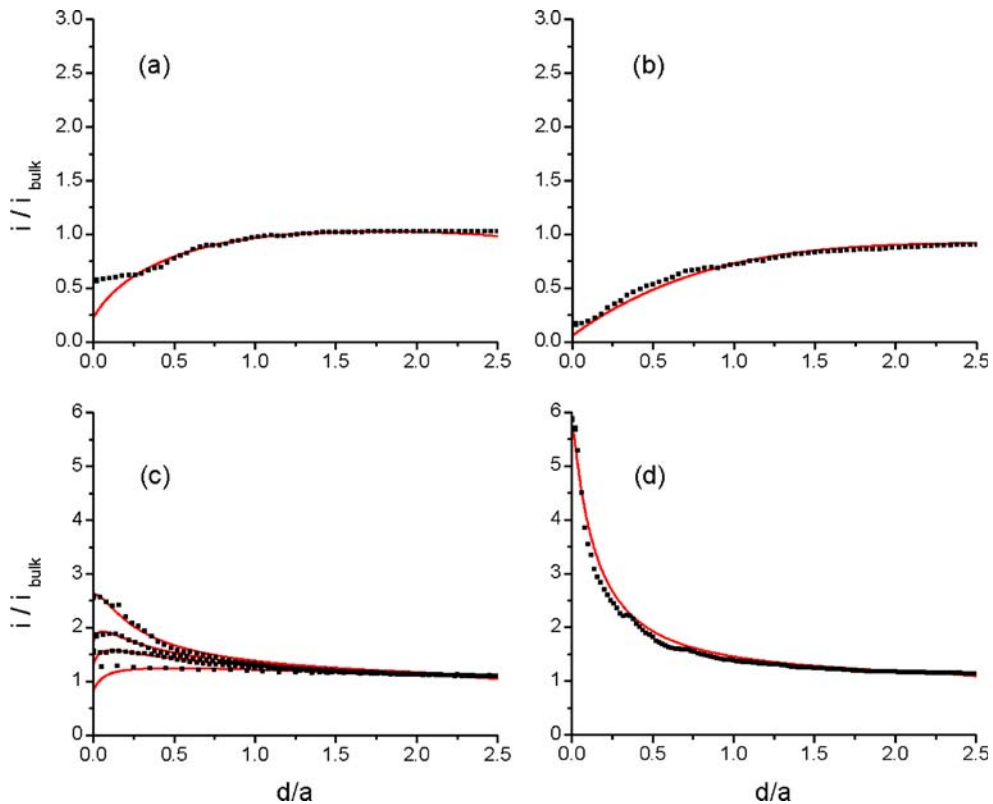


Table 2 Values of the apparent heterogeneous electron rate transfer values (k_{app}) on ITO and BDD electrodes for different mediator species

Mediator species in the bulk	Electrode material	
	ITO k_{app} (cm s ⁻¹)	BDD k_{app} (cm s ⁻¹)
Ru(CN) _{6(aq)} ⁴⁻	0.073	0.012–0.036
FeMeOH	0.004	0.004–0.013
Fe(CN) _{6(aq)} ³⁻	0.021	0.001–0.006
Ru(NH ₃) _{6(aq)} ³⁺	0.125	0.079–0.140

order of the most positive standard potential to the least. Probing different regions on the ITO surface, either by the approach curve method or by performing a linescan at a constant height, resulted in indistinguishable data for each mediator. Hence, it was deduced for ITO that its physical structure was highly uniform and our simple cleaning procedure did not chemically alter the surface.

Use of mixed mediators on ITO

Approach curve experiments were carried out at ITO electrodes using mixtures of Fe(CN)_{6(aq)}³⁻ and Fe(CN)_{6(aq)}⁴⁻ mediators, and hence, the potential of the ITO electrode was then controlled indirectly by varying their concentration ratio. Illustrated in Fig. 4 is a plot of the OCP recorded at an ITO electrode vs $\log ([\text{Fe}(\text{CN})_{6(aq)}^{3-}] / [\text{Fe}(\text{CN})_{6(aq)}^{3-}])$. It can be seen quite clearly that there is a near-Nernstian response for this system. Illustrated in Fig. 5 are approach curves using Fe(CN)_{6(aq)}³⁻ and Fe(CN)_{6(aq)}⁴⁻ mediators at different concentration

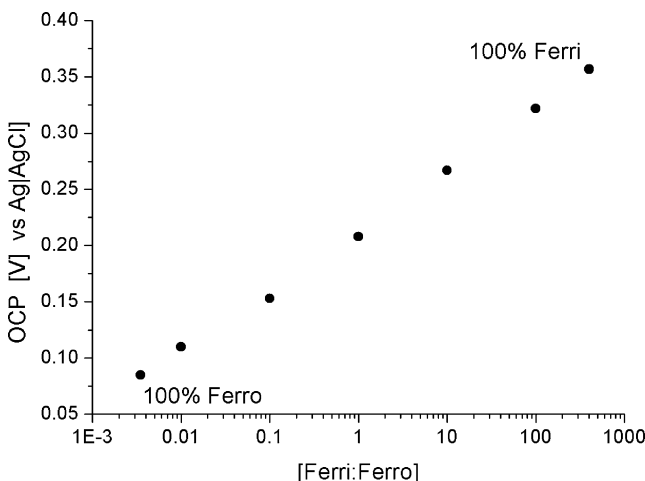


Fig. 4 Graph of the OCP of ITO vs Ag|AgCl when exposed to deaerated solutions of 1 mM ferricyanide, 1 mM ferrocyanide, and 100:1, 10:1 and 1:1 mixtures

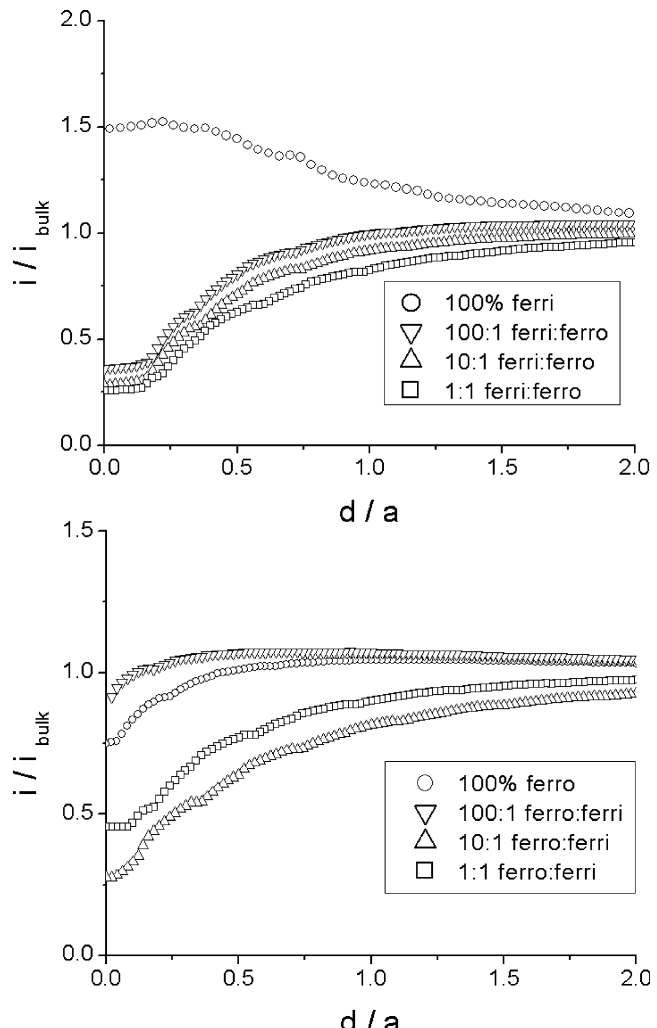


Fig. 5 Approach curve graphs obtained in feedback mode using the mediator ferricyanide, ferrocyanide at a concentration of 1 mM and mixtures of both (100:1, 10:1 and 1:1) on an ITO electrode. k_{app} values for ferrocyanide additions to ferricyanide (top) range from 0.003 to 0.021 cm s⁻¹, and for ferricyanide additions to ferrocyanide (bottom), from 0.003 to 0.010 cm s⁻¹. Comparison of pure ferrocyanide to ferricyanide: 0.007 to 0.021 cm s⁻¹

ratios. Taking the Fe(CN)_{6(aq)}³⁻ case, it is quite clear that the extent of feedback recorded is highly inhibited by the presence of Fe(CN)_{6(aq)}⁴⁻ in solution. As can be seen from Fig. 4, the presence of Fe(CN)_{6(aq)}⁴⁻ lowers the OCP at ITO and the driving force for the re-oxidation of the electrogenerated mediator at the ITO electrode. A similar trend is found for Fe(CN)_{6(aq)}⁴⁻ containing additions of Fe(CN)_{6(aq)}³⁻; however, the extent of inhibition is not as dramatic when compared to the latter case, particularly when low levels (1%) of Fe(CN)_{6(aq)}³⁻ are present. It is noteworthy that a higher k_{app} value was observed (0.021 compared to 0.007 cm s⁻¹) when Fe(CN)_{6(aq)}³⁻ is used as a mediator that probes an electron injection process into ITO, compared to Fe(CN)_{6(aq)}⁴⁻, which probes electron withdrawal (as illustrated generally in Fig. 1).

Variation of the mediator on BDD

On BDD, quite a different result was obtained in comparison to the uniform ITO surface. For each mediator, although near identical approach curves were obtained at a single location on the substrate, when moving to a new region quite different approach curve data were obtained and, hence, a range of values for k_{app} . Figure 3 shows experimental and modelled approach curves for each of the mediators, with multiple experimental approach curves and modelled data only shown for the mediator $\text{Ru}(\text{CN})_{6(aq)}^{4-}$. In the same order of mediators as listed above for ITO (most to least positive reversible potential), the range of k_{app} values for BDD are 0.012–0.36, 0.004–0.13, <0.001–0.006 and 0.079–0.140 cm s^{-1} . Variation in the feedback response observed spatially over the BDD surface was further confirmed by performing a linescan (Fig. 6). In this experiment, the UME is traversed at a constant distance from the surface, and the feedback current at the tip is recorded. It should be noted that the BDD material used in our study was highly polished and had a roughness less than one third that of the ITO surface. Using data obtained from contact mode AFM, for ITO the roughness measure (R_a) was 6.7 nm, and for BDD, 2.2 nm. To complete the data set, the surface was mapped in feedback mode (Fig. 7). In this figure, a colour platelet has been used to emphasise the regions of significant positive feedback (red and yellow), regions of near unity feedback (green) and slightly less (blue) on a normalised scale. A region similar in size (100 by 100 microns) was inspected using AFM, and the greatest change in height in the image was about 35 nm. The combination of approach curve data (height independent) and the topographic data obtained by

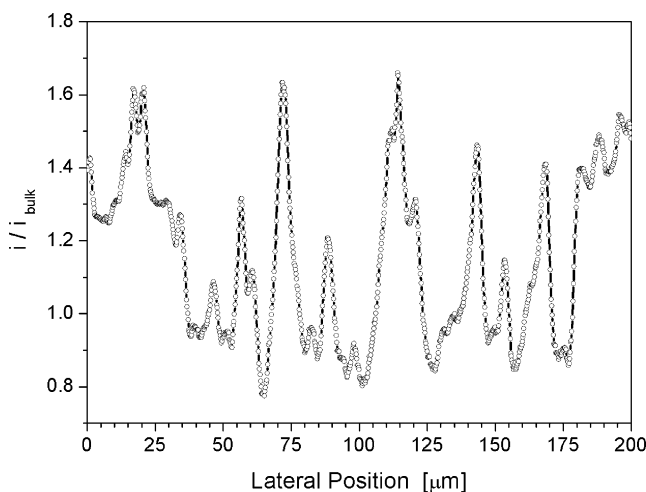


Fig. 6 Data collected in feedback mode with the mediator $\text{Ru}(\text{NH}_3)_{6(aq)}^{3+}$ at a concentration of 1 mM by traversing at Pt UME (2 μm in diameter) at $5 \mu\text{m s}^{-1}$ above the surface of BDD at a height of approximately 2 μm

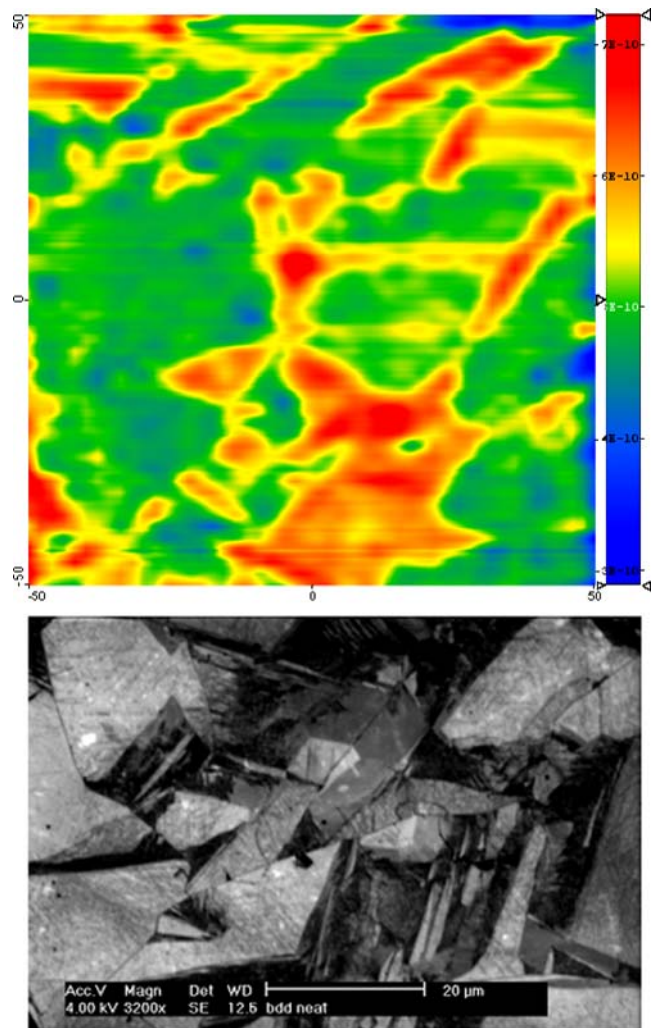
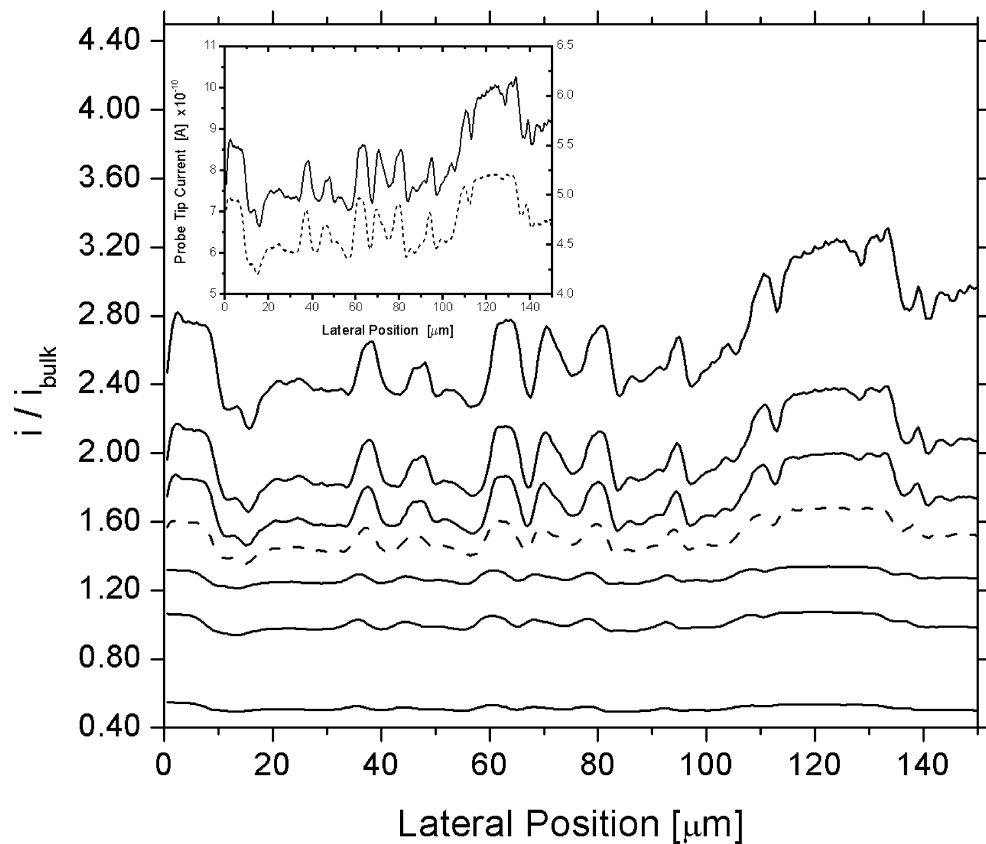


Fig. 7 Images of the surface of a BDD electrode generated using (top) feedback mode SECM and (bottom) secondary electron detector on a scanning electron microscope. SECM map (100x100 μm) obtained with the mediator $\text{Ru}(\text{NH}_3)_{6(aq)}^{3+}$ at a concentration of 1 mM using a Pt UME (2 μm in diameter) at a tip–substrate separation of approximately 2 μm . Lateral scan rate 5 $\mu\text{m s}^{-1}$

AFM quite strongly confirms that the variations observed in the SECM-generated data in Figs. 6 and 7 are not due to topographic effects. Hence, these changes in feedback signal are most likely due to variations in the electronic conductivity between grains that are highly doped in boron and grains that are not. Supporting this is the micrograph of the BDD electrode surface obtained by SEM. Being that the electrode is entirely composed of carbon, it is well known that darker areas in the image are formed by more conductive regions and the white areas by more insulating regions. By comparison, it is plainly clear that there is a striking variation in the electrochemical activity of the surface (SECM map) that corresponds to small regions or grains that compose the surface of varying electronic properties [43] (SEM image).

Fig. 8 Constant height data using 1 mM of the mediator $\text{Ru}(\text{NH}_3)_6^{3+}$ in feedback mode over BDD electrode. *Solid line* traces are from experiments where the substrate voltage was varied from 0.20 to -0.015 V; the *dashed line* was obtained at OCP in feedback mode. *Inset:* comparison of data obtained at 0.20 V and at OCP with expansion of each axis. *Solid traces* from top to bottom are 0.20, 0.10, 0.05, 0, -0.01 and -0.15 V vs Ag|AgCl. Obtained using a Pt UME (2 μm diameter) at a tip-substrate separation of 2.1 μm and a lateral scan rate of 2.5 $\mu\text{m s}^{-1}$



Performing feedback mode with biased BDD

With the striking variations observed spatially on BDD at OCP, we found it intriguing to perform a linescan experiment using the mediator $\text{Ru}(\text{NH}_3)_6^{3+}$ and varying the potential of this heterogeneous material. Figure 8 show traces from experiments conducted at a range of potentials, including at OCP (see figure caption for values). Not surprising is the variation in the magnitude of the feedback current measured at the UME tip with BDD under potential control; however, it does appear, by closer inspection of the trace obtained at OCP with that obtained at 0.2 V (see Fig. 8 inset), that the variations in feedback observed are nearly identical. These data imply that when using

$\text{Ru}(\text{NH}_3)_6^{3+}$ as a mediator on BDD, there is no apparent effect of the thermodynamic driving force on the rate of charge transfer, i.e. new electrochemically active states are not accessed under potential control.

Further considerations

The properties of a semiconductor substrate at OCP that will influence the feedback response are the concentration of charge carriers in the bulk and their mobility, the existence of surface states and the chemical nature of the surface. The concentration of charge carriers and their mobility will govern the nature of the space charge layer, as will the position of the Fermi energy relative to the band

Fig. 9 Electronic energy band diagrams for the interaction of ITO and charge carriers with mediators **a** $\text{Ru}(\text{CN})_6^{4-}$ within the bandgap and **b** near the conduction band edge (E_{CB}) and with $\text{Ru}(\text{NH}_3)_6^{3+}$. The process in **b** is very efficient

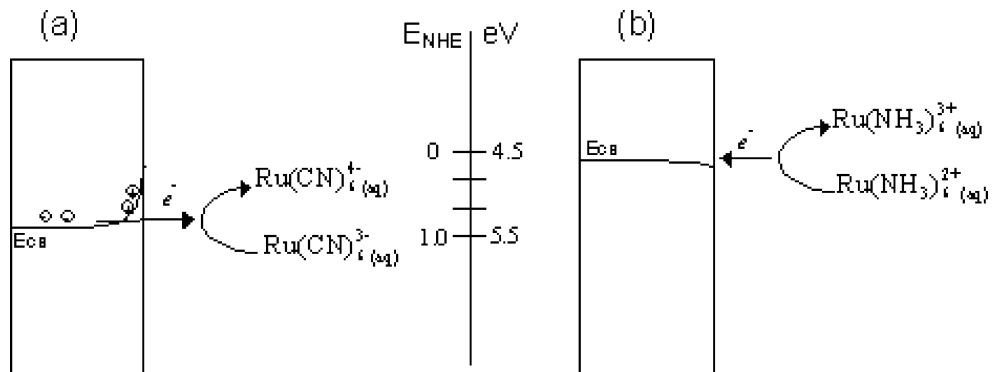
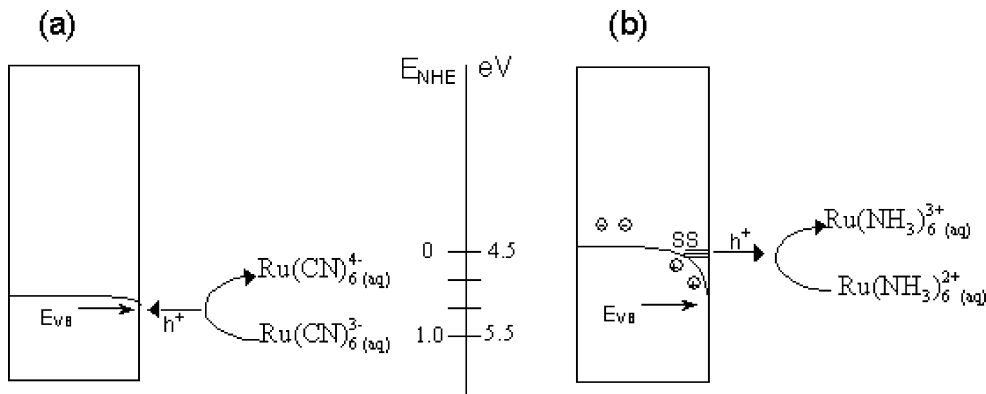


Fig. 10 Electronic energy band diagrams for the interaction of BDD with mediators **a** $\text{Ru}(\text{CN})_{6(\text{aq})}^{4-}$ near the valence band edge (E_{VB}) and **b** $\text{Ru}(\text{NH}_3)_{6(\text{aq})}^{3+}$. Oxidation of $\text{Ru}(\text{NH}_3)_{6(\text{aq})}^{3+}$ unexpectedly occurs by h^+ transfer from the valence band via surface states (SS)



edges. By changing the mediator, the potential at which the density of states of the redox species relative to the majority carrier band edge changes; therefore, we change the degree of band bending and, in some cases, significantly alter the nature of the space charge layer [49]. Figure 9 depicts an energy band diagram for charge transfer between ITO and the redox species $\text{Ru}(\text{NH}_3)_{6(\text{aq})}^{3+/2+}$ and $\text{Ru}(\text{CN})_{6(\text{aq})}^{4-/3-}$ in the immediate vicinity of the UME. For the $\text{Ru}(\text{NH}_3)_{6(\text{aq})}^{3+/2+}$, which is positioned energetically [50] near the conduction band edge (for ITO the fermi level may actually reside within the conduction band), charge transfer is relatively facile compared to $\text{Fe}(\text{CN})_{6(\text{aq})}^{3-/4-}$ and $\text{FcMeOH}_{(\text{aq})}^{0/+}$, which most likely are positioned within the band gap. For $\text{Ru}(\text{CN})_{6(\text{aq})}^{4-/3-}$, we hypothesise that electron tunneling occurs with such severe band bending [50]. On BDD, similar simple energy band diagrams [45] may be drawn (Fig. 10); however, the explanation of the variation in k_{app} is twofold. Firstly, differences in k_{app} values obtained for different mediators are similar as for ITO; however, the charge carriers are holes instead of electrons. Nevertheless, we anticipate the effect of positioning of the mediators' reversible potential within the band gap of the BDD will be similar. The measurement of a relatively high degree of feedback using the mediator $\text{Ru}(\text{NH}_3)_{6(\text{aq})}^{3+}$ is unexpected. Depicted in Fig. 10 is the interaction of this mediator with a surface state, most likely some manifestation of boron doping of the diamond material [45].

Conclusions

ITO and BDD have been examined in detail using the SECM technique in feedback mode. For interrogation of these electrodes, the use of the mediators $\text{Ru}(\text{CN})_{6(\text{aq})}^{4-}$, ferrocene methanol (FcMeOH), $\text{Fe}(\text{CN})_{6(\text{aq})}^{3-}$ and $\text{Ru}(\text{NH}_3)_{6(\text{aq})}^{3+}$ has been successful in gaining insights into the nature of charge transfer at these electrode surfaces. Calculations of the apparent heterogeneous electron transfer rates (k_{app}) using data from approach curve experiments assist in understanding the possible effect that the semiconductor energy band

structure may have on charge transfer. For ITO, the feedback responses in terms of k_{app} are 0.073, 0.004, 0.021 and 0.125 cm s^{-1} for the mediators in the order of the most positive standard potential to the least. For BDD, the ranges of k_{app} values are 0.012–0.36, 0.004–0.13, <0.001–0.006 and 0.079 – 0.140 cm s^{-1} . The variation in the feedback response observed spatially over the extremely flat BDD surface was further confirmed by performing a linescan and a map. On the BDD electrode, the use of the mediator $\text{Ru}(\text{CN})_{6(\text{aq})}^{4-}$ results in positive feedback as expected; it is, however, with the mediator $\text{Ru}(\text{NH}_3)_{6(\text{aq})}^{3+}$ that the highest k_{app} value is observed. This is despite the fact that $\text{Ru}(\text{NH}_3)_{6(\text{aq})}^{3+}$ has a reversible potential more negative than the equivalent energy level of the anticipated valence band edge and is most likely due to electron transfer through surface states of the BDD.

Acknowledgements A.K. Neufeld gratefully acknowledges Alan Bond for his friendship, bright enthusiasm and subtle guidance. The authors thank Steven Feldberg and Jie Zhang for insightful comments and J. Ward for assistance in access to SEM facilities. Financial support by Commonwealth Scientific & Industrial Research Organization division of Manufacturing and Infrastructure Technology and the Australian Research Council is also gratefully acknowledged.

References

1. Csóka B, Kovács B, Nagy G (2003) *Electroanalysis* 15:1335
2. Takai Y, Takoh K, Nishizawa M, Matsue T (2003) *Electrochim Acta* 48:3381
3. Kaya T, Torisawa Y-S, Oyamatsu D, Nishizawa M, Matsue T (2003) *Biosens Bioelectron* 18:1379
4. Kranz C, Wittstock G, Wohlschläger H, Schuhmann W (1997) *Electrochim Acta* 42:3105
5. Barker AL, Unwin PR, Zhang J (2001) *Electrochim Commun* 3:372
6. Zhou J, Zu Y, Bard AJ (2000) *J Electroanal Chem* 491:22
7. Wijayawardhana CA, Wittstock G, Halsall HB, Heineman WR (2000) *Electroanalysis* 12:640
8. Wittstock G, Wilhelm T, Bahrs S, Steinrücke P (2001) *Electroanalysis* 13:669
9. Yasukawa T, Kaya T, Matsue T (2000) *Electroanalysis* 12:653

10. Fernandez JL, Walsh DA, Bard AJ (2005) *J Am Chem Soc* 127:357
11. Kallio T, Slevin C, Sundholm G, Holmlund P, Kontturi K (2003) *Electrochim Commun* 5:561
12. Nugues S, Denuault G (1996) *J Electroanal Chem* 408:125
13. Schulte A, Belger S, Etienne M, Schuhmann W (2004) *Mater Sci Eng A* 378:523
14. Souto RM, Gonzalez-Garcia Y, Gonzalez S, Burstein GT (2004) *Corros Sci* 46:2621
15. Semenikhin OA, Stromberg C, Ehrenburg MR, König U, Schultze JW (2001) *Electrochim Acta* 47:171
16. O'Mullane A, Neufeld AK, Bond AM (2005) *Anal Chem* 77:5447
17. Ufheil J, Boldt FM, Börsch M, Borgwarth K, Heinze J (2000) *Bioelectrochemistry* 52:103
18. Neufeld AK, O'Mullane AP, Bond AM (2005) *J Am Chem Soc* 127:13846
19. Martin RD, Unwin PR (1997) *J Electroanal Chem* 439:123
20. Rajendran L, Ananthi SP (2004) *J Electroanal Chem* 561:113
21. Wipf DO, Bard AJ (1991) *J Electrochim Soc* 138:469
22. Kwak J, Bard AJ (1989) *Anal Chem* 61:1221
23. Mirkin MV, Horrocks BR (2000) *Anal Chim Acta* 406:119
24. Pleskov YV (2002) *Russ J Electrochim* 38:1049
25. Combelles C, Kanoufi F, Mazouzi D, Thiébault A (2003) *J Electroanal Chem* 556:43
26. Goeting CH, Marken F, Compton RG, Foord JS, Salter C (1999) *Chem Commun* 1999:1697
27. Mandler D, Bard AJ (1989) *J Electrochim Soc* 136:3143
28. Wilhelm T, Wittstock G (2001) *Electrochim Acta* 47:275
29. Mukhopadhyay I, Aravinda CL, Borissov D, Freyland W (2005) *Electrochim Acta* 50:1275
30. Compton RG, Foord JS, Marken F (2003) *Electroanalysis* 15:1349
31. Fortin E, Chane-Tune J, Mailley P, Szunerits S, Marcus B, Petit J-P, Mermoux M, Vieil E (2004) *Bioelectrochemistry* 63:303
32. Chatterjee A, Compton RG, Foord JS, Hiramatsu M, Marken F (2003) *Phys Status Solidi* 199:49
33. Fischer AE, Show Y, Swain GM (2004) *Anal Chem* 76:2553
34. Haymond S, Babcock GT, Swain GM (2003) *Electroanalysis* 15:249
35. Holt KB, Bard AJ, Show Y, Swain GM (2004) *J Phys Chem B* 108:15117
36. Wang K, Xu J-J, Sun D-C, Wei H, Xia X-H (2005) *Biosens Bioelectron* 20:1366
37. Popovich ND, Wong S, Ufer S, Sakhrani V, Paine D (2003) *J Electrochim Soc* 150:H255
38. Popovich ND, Wong S, Yen BKH, Yeom H-Y, Paine D (2002) *Anal Chem* 74:3127
39. Shen Y, Jacobs DB, Malliaras GG, Koley G, Spencer MG, Ioannidis A (2001) *Adv Mater* 13:1234
40. Chiguvare Z, Parisi J, Dyakonov V (2003) *J Appl Phys* 94:2440
41. Goeting CH, Marken F, Gutierrez-Sosa A, Compton RG, Foord JS (2000) *Diam Relat Mater* 9:390
42. Granger MC, Swain GM (1999) *J Electrochim Soc* 146:4551
43. Wilson NR, Clewes SL, Newton ME, Unwin PR, Macpherson JV (2006) *J Phys Chem B* 110:5639
44. Colley AL, Williams CG, Johansson UD, Newton ME, Unwin PR, Wilson NR, Macpherson JV (2006) *Anal Chem* 78:2539
45. Latto MN, Pastor-Moreno G, Riley DJ (2004) *Electroanalysis* 16:434
46. Mirkin MV, Fan F-RF, Bard AJ (1992) *J Electroanal Chem* 328:47
47. Wei C, Bard AJ (1995) *J Electrochim Soc* 142:2523
48. Bard AJ, Mirkin MV (eds) (2001) *Scanning electrochemical microscopy*. Marcel Dekker, New York
49. Oskam G, Long JG, Natarajan A, Searson PC (1998) *J Phys D Appl Phys* 31:1927
50. Sato N (1998) *Electrochemistry at metal and semiconductor electrodes*. Elsevier, Amsterdam